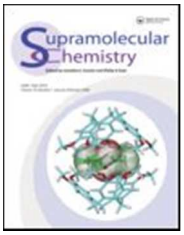

Multiple inclusion complex formation of protonated ellipticine with cucurbit[8]uril: Thermodynamics and fluorescence properties

Journal:	*Supramolecular Chemistry*
Manuscript ID	GSCH-2015-0254.R2
Manuscript Type:	Special Issue Paper
Date Submitted by the Author:	n/a
Complete List of Authors:	Miskolczy, Zsombor; Research Centre for Natural Sciences Hungarian Academy of Sciences Biczók, László; Research Centre for Natural Sciences Hungarian Academy of Sciences, Jablonkai, István; Research Centre for Natural Sciences Hungarian Academy of Sciences
Keywords:	alkaloids, calorimetry, fluorescence decay, host-guest complex, binding affinity

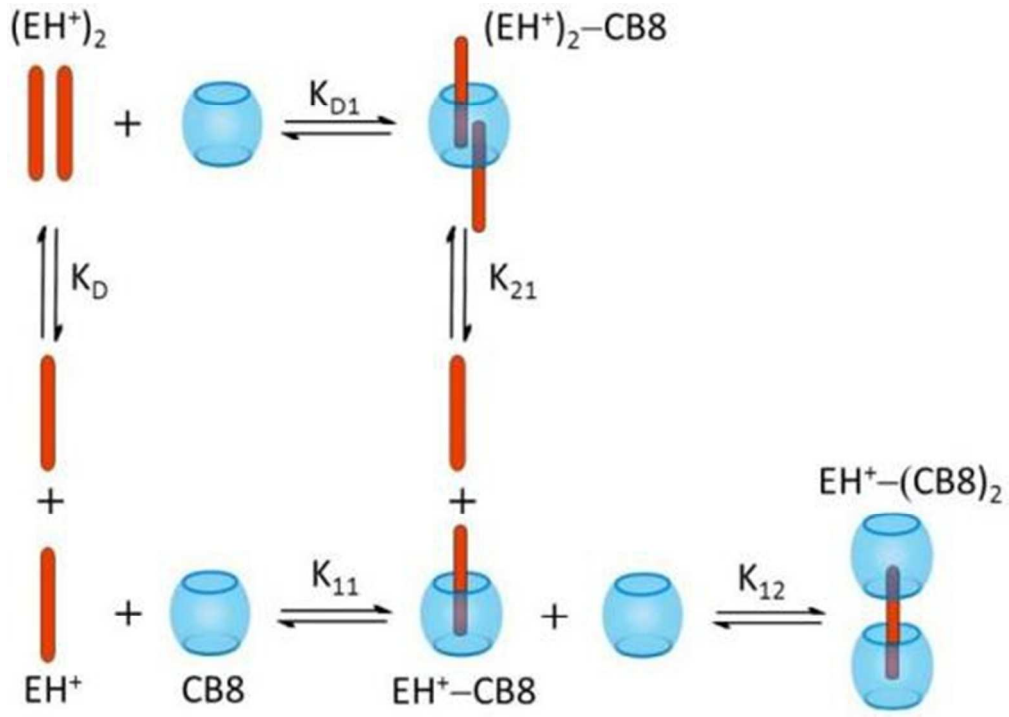

60x43mm (220 x 220 DPI)

Multiple inclusion complex formation of protonated ellipticine with cucurbit[8]uril: Thermodynamics and fluorescence properties

Zsombor Miskolczy,[a] László Biczók[a*], István Jablonkai[b]

[a]*Institute of Materials and Environmental Chemistry, Research Centre for Natural Sciences, Hungarian Academy of Sciences, P.O. Box 286, 1519 Budapest, Hungary*

[b]*Institute of Organic Chemistry, Research Centre for Natural Sciences, Hungarian Academy of Sciences, P.O. Box 286, 1519 Budapest, Hungary*

This work was supported by the Hungarian Scientific Research Fund (OTKA) under Grant K104201, MedInProt Protein Science Research Synergy Program, and János Bolyai Research Scholarship of the Hungarian Academy of Sciences.

[*] Corresponding author. E-mail: biczok.laszlo@ttk.mta.hu

ABSTRACT

The encapsulation of protonated ellipticine (EH^+) in the cavity of cucurbit[8]uril (CB8) was studied in water at pH 4 with spectrophotometric, fluorescence spectroscopic and isothermal calorimetric measurements. The formation of three types of inclusion complexes was observed depending on the host and guest concentrations. Not only one but also two EH^+ was capable of encapsulation in CB8 in 37 μM EH^+ solution and the thermodynamics of the binding steps were revealed. The produced very stable complexes showed markedly different absorption and fluorescence properties. When large excess of CB8 was employed in dilute (0.49 μM) EH^+ solution, sequential binding of two CB8 occurred to the monomer alkaloid bringing about a substantial alteration in the fluorescence decay kinetics. The driving force of the 1:2 guest:host complex formation was much lower than that of 1:1 encapsulation.

Key words: alkaloids, calorimetry, fluorescence decay, host-guest complex, binding affinity

1. Introduction

The inclusion complex formation of cucurbiturils (CBn) with compounds of pharmaceutical importance has attracted widespread attention because of its great potential in drug delivery (1-4) and development of sensitive analytical methods (5-8). These macrocyclic hosts are nontoxic and capable of traversing the cell membrane (9-11). The confinement of drugs in CBn cavity not only enhances the solubility (12,13) and thermal stability (14), but also hinders the decomposition (15,16). For example, the nucleophilic addition reaction and photooxidation of sanguinarine, a biologically active natural benzophenanthridine alkaloid, are inhibited by the embedment in cucurbit[7]uril (CB7) macrocycle (17). The microenvironment-sensitive fluorescent properties of berberine were used to examine the encapsulation and dissociation kinetics with CBn cavitands (18,19).

Due to its anticancer (20) and antimalarial (21) activity, ellipticine (E) has been extensively investigated, and the intricate mechanism of its biological effect has been revealed (22). E has a very low water solubility of ~6.2×10^{-7} M at neutral pH (23,24), but more than 3 orders of magnitudes higher concentration can be the reached upon the protonation of the pyridine moiety. The conjugate acid has a pK_a value of 7.4 ± 0.1 in 0.025 M buffers (25). The fluorescent behavior of E was examined in organic solvents of a wide range of polarities and hydrogen bonding capabilities (26). The effect of interaction between the NH group of E and hydrogen bond acceptors on the absorption and fluorescence characteristics was revealed. Photoinduced deprotonation was found in acetonitrile only with a very strong base, 1,8-diazabicyclo[5.4.0]undec-7-ene (DBU), due to the extremely weak acidity of the NH moiety of E even in the singlet-excited state (27). Therefore, photoinitiated tautomerization via intramolecular proton transfer from the pyrrolic NH to the nitrogen of the pyridine ring cannot occur. The lack

of such a tautomerization was proved by the analogous fluorescence properties of E and its 6-methyl derivative (ME), which does not contain any dissociable hydrogen (28,29).

The encapsulation of the protonated form of ellipticine (EH^+) in cucurbiturils has been examined, and only 1:1 complex formation was reported with both CB7 and cucurbit[8]uril (CB8) despite the substantial change of the fluorescence decay parameters upon gradual increase of host concentration (30). The main goals of the present studies were to understand the CB8 concentration dependence of the kinetics of EH^+ fluorescence and to identify the various fluorescent species. We reveal how the amounts of EH^+ and CB8 in the solutions affect the stoichiometry and thermodynamics of inclusion complex formation. The formulae of the investigated compounds are presented in Figure 1.

2. Experimental

Ellipticine (≥99% by HPLC, Fluka) was used as received. High-purity CB8 was kindly provided by Dr Anthony I. Day (University of New South Wales, Canberra, Australia). Experiments were performed in double-distilled water at pH 4. Slightly more than stoichiometric amount of concentrated HCl aqueous solution was added to ellipticine in ethanol. The solvent and the excess of HCl were evaporated. EH^+Cl^- salt prepared thereby was dissolved in 10^{-4} M HCl aqueous solution. The UV-visible absorption spectra were measured on an Agilent Technologies Cary60 spectrophotometer. Corrected fluorescence spectra were recorded on a Jobin-Yvon Fluoromax-4 photoncounting spectrofluorometer. No photodecomposition occurred when EH^+ aqueous solutions were irradiated in the sample holder of the spectrofluorometer in the presence and absence of CB8. Fluorescence decays were collected with time-correlated single-photon counting technique using the previously described instrument (31). The results of spectrophotometric and fluorescence titrations were analysed with homemade programs written

in MATLAB 7.9 analogously to that reported in a former paper (31). Starting with the initial estimates of the binding constant, the concentrations of the various species were calculated as numerical solutions of the mass balance equations and the definition of the binding constants. Then, the fluorescence intensity or absorbance values were calculated, and the iterations were repeated until the best fit was achieved. Isothermal titration calorimetry was carried out with a VP-ITC (MicroCal) instrument at 298 K as described (19).

3. Results

3.1 Inclusion complex formation with CB8 at low EH^+ concentration

To avoid dimerization, 0.49 μM total protonated ellipticine concentration was used in the study of the interaction with CB8. Calculations using the recently published dimerization constant ($(1.4 \pm 0.3) \times 10^4$ M^{-1}) showed that less than 2% of the alkaloid molecules are associated in such a dilute solution (32). Gradual addition of CB8 to EH^+ solution at pH 4 brought about an intensity enhancement and a hypsochromic shift in the fluorescence spectrum indicating complex formation (Figure 2A). The plot of the intensity at 530 and 560 nm as a function of CB8 concentration exhibits two distinct domains. The steep initial rise is followed by a much slower intensity enhancement suggesting sequential binding of two CB8 cavitands. The equilibrium constants are defined as

$$K_{11} = \frac{[EH^+{-}CB8]}{[EH^+][CB8]} \quad (1)$$

$$K_{12} = \frac{[EH^+{-}(CB8)_2]}{[EH^+{-}CB8][CB8]} \quad (2)$$

The results presented in Figure 2B were analysed by a previously described homemade MATLAB 7.9 program (31). The nonlinear fit provided K_{11} = $(1.6 \pm 0.2)\times10^6$ M^{-1} and K_{12} = $(5\pm4)\times10^3$ M^{-1}, whereas the fluorescence efficiency at 560 nm was about 5-fold larger for 1:2

EH^+–$(CB8)_2$ complex than that of 1:1 EH^+–CB8 complex. The microenvironment of the guest is less polar in EH^+–$(CB8)_2$ than in water analogously to previous findings (33). Therefore, blue-shift is observed in the fluorescence spectrum with the increase of CB8 concentration. Time-resolved fluorescence measurements at 590 nm corroborated the formation of two types of inclusion complexes. As expected, the amplitude of the dimer fluorescence was negligible (< 2%) in 0.49 μM EH^+ solution. The fluorescence decays could be fitted by a triple-exponential function:

$$I(t) = a_1 \exp\left(-\frac{t}{\tau_1}\right) + a_2 \exp\left(-\frac{t}{\tau_2}\right) + a_3 \exp\left(-\frac{t}{\tau_3}\right) \quad (3)$$

where a_i stands for the amplitudes and τ_i denotes the lifetimes. Figure 3 shows the variation of the amplitude fractions (a_i /Σa_i) in the presence of various amounts of CB8. The monomer fluorescence of 2.0 ns lifetime vanished in the presence of large CB8 excess and the concomitant emergence of a 3.8 ns lifetime component was observed, which was assigned to singlet-excited EH^+–CB8. The amplitude of this emission (a_2) reached a maximum around 7 μM CB8 concentration and then declined due to the progressive strengthening of a third component of 16.6 ns lifetime. The longest-lived fluorescence was attributed to EH^+–$(CB8)_2$ because its amplitude (a_3) grew at the expense of a_2 at high CB8 concentrations. The substantial difference in the initial slope of a_2 and a_3 increase is in accordance with the more than two orders of magnitude larger equilibrium constant of EH^+–CB8 formation compared to that of the binding of the second CB8.

To reveal the thermodynamics of EH^+ inclusion in CB8, the fluorescence titrations displayed in Figure 2 were repeated at various temperatures (T). The van't Hoff plot of the derived K_{11} binding constant is presented in Figure 4. From the slope and intercept, $\Delta H_{11} = -20 \pm 3$ kJ mol^{-1} and $\Delta S_{11} = 51 \pm 7$ J mol^{-1} K^{-1} were calculated for the enthalpy and

entropy change in 1:1 host–guest complex formation. The thermodynamic parameters of CB8 association with EH^+–CB8 could not be obtained due to the substantial uncertainty of K_{12}.

3.2 Binding to CB8 at high EH^+ concentration

Intriguing absorption and fluorescence characteristics was observed in CB8 solutions containing 37 μM total EH^+ concentration. Under this condition, 38% of alkaloid molecules are dimerized in the absence of CB8 on the basis of the recently reported association constant of ((K_D =1.4 ± 0.3)×10^4 M^{-1}) (32). Figure 5 displays the change of the absorption spectra and the absorbance at 327 nm upon increase of the amount of CB8 in the solution. The experimental data demonstrate that different species dominate at 22 and 97 μM CB8 concentrations. This conclusion was corroborated by the results of fluorescence titration. (Figure 6) The apparent blue shift of the fluorescence maximum in the presence of 97 μM CB8 originated from the dissociation of the $(EH^+)_2$ dimer upon complex formation with CB8. To identify the binding processes, fluorescence decay measurements were performed at 530 nm. The biexponential fluorescence intensity versus time profile arising from monomer and dimer EH^+ became triple exponential in the presence of CB8. Below 30 μM CB8 concentration, lifetimes of 2.0, 3.8, and 7.5 ns were found. Upon further addition of CB8, EH^+ emission vanished, and a very weak emission of 16.6 ns lifetime emerged. The 2.0, 3.8 and 16.6 ns lifetimes have been ascribed to monomer EH^+, EH^+–CB8, and EH^+–$(CB8)_2$ fluorescence, respectively. (vide supra) These assignments are corroborated by the variation of the amplitude fractions displayed in Figure 7.

The intensity of 2.0 ns lifetime component progressively diminishes and disappears above 30 μM CB8 concentration because all EH^+ ions are encapsulated. This trend is accompanied by the parallel growth of the amplitude fraction of EH^+–CB8 emission (τ_2 = 3.8 ns), which dominates at high CB8 concentrations. The EH^+–$(CB8)_2$ fluorescence component

(τ_3 = 16.6 ns) is much weaker than at low EH^+ concentration because of the smaller molar excess of CB8. The amplitude of 7.5 ns emission goes through a maximum as a function of CB8 concentration implying the formation of $(EH^+)_2$–CB8 and its conversion into EH^+–CB8. The confinement in CB8 insignificantly affects the fluorescence lifetime of $(EH^+)_2$. No evidence was found for 2:2 binding. The Job plot of the absorbance change is presented in Figure S1 in Supporting Information. Among the experimentally detected species, the following association equilibriums are possible: (Figure 8)

Because the fluorescence decay traces showed very small amounts of EH^+–$(CB)_2$ in 37 μM EH^+ solution over the entire CB8 concentration range, its formation was neglected in the evaluation of the experimental data presented in Figures 5 and 6. Our goal was to reveal the binding equilibriums resulting in $(EH^+)_2$–CB8. This ternary complex may be produced (i) by consecutive binding of two EH^+ in CB8, (ii) by direct inclusion of $(EH^+)_2$ dimer or (iii) both processes may take place. First, we assumed that consecutive binding of two EH^+ occurs. The reaction between $(EH^+)_2$ and CB8 was eliminated and the experimental data were fitted with a MATLAB program developed on the basis of the remaining equilibriums. K_{11} was known from the independent experiments at 0.49 μM EH^+ concentration, whereas the molar absorption coefficient ratio at 327 nm ($\varepsilon((EH^+)_2)/\varepsilon(EH^+)$ = 3.52) and the relative fluorescence efficiency at 530 nm ($f((EH^+)_2)/f(EH^+)$ = 2.10) for $(EH^+)_2$ and EH^+ as well as the association constant of $(EH^+)_2$ dimer formation, K_D were taken from measurements carried out in the absence of CB8. The nonlinear regression analysis of the spectrophotometric and fluorescence titration data at 37 μM EH^+ concentration gave $K_{21} = (4.2 \pm 0.8) \times 10^4$ M^{-1} and the computed functions matched the experimental data well (insets to Figures 5 and 6).

In the second step, we assumed that $(EH^+)_2$–CB8 is formed only in the association of $(EH^+)_2$ with CB8. Thus, the complex formation between EH^+ and EH^+–CB8 was eliminated. Excellent fit was obtained, and $K_{D1} = (5.2 \pm 0.95) \times 10^6$ M^{-1} was found for the equilibrium constant of $(EH^+)_2$ dimer confinement in CB8. This K_{D1} value corresponded to that calculated using K_{21}, K_{11}, and K_D values given in Table 1 by the relationship

$$K_{D1} = K_{21}K_{11}/K_D \quad (4)$$

Supporting Information shows the derivation of eq 4. This relationship is valid if the cycle of equilibriums shown in Figure 8 exists. The good match of the K_{D1} value obtained in the second analysis step and K_{D1} derived by eq 4 indicates that not only the consecutive encapsulation of two EH^+ but also the direct $(EH^+)_2$–CB8 formation with the interaction of $(EH^+)_2$ and CB8 occur. The calculated binding constants are summarized in Table 1.

NMR measurements in the presence of 190 μM CB8 confirmed the inclusion complex formation. Higher CB8 concentration could not be employed because of the low solubility of CB8 even in the presence of EH^+. The NMR spectra are displayed in Figure S4 in Supporting Information.

3.3 Determination of the thermodynamic parameters of inclusion at high EH^+ concentration

Isothermal calorimetric measurements at pH 4 gave information on the thermodynamics of complex formation. Figure S2 in Supporting Information displays the experimental results for the titration of 124 μM CB8 to 8.0 μM EH^+ solution at 298 K. Exothermic complexation was observed. The data were consistent with a sequential binding to two sites model. To decrease the number of fitted parameters, K_{11} and K_{21}, were taken from Table 1 and kept constant. The nonlinear least-squares analysis led to the thermodynamic quantities listed in Table 2.

To verify the calorimetric results, the spectrophotometric titrations presented in Figure 5 were repeated at various temperatures. At each temperature the experimental data were fitted keeping K_{11} and K_D fixed at the value calculated on the basis of the calorimetric determined enthalpy and entropy changes. ΔH and ΔS for the formation of EH^+–CB8 is given in Table 2, whereas these quantities for EH^+ dimerization were taken from a recent paper (32). The van't Hoff plot of the calculated K_{21} binding constants is shown in Figure S3 in Supporting Information. The thermodynamic parameters derived therefrom are included in Table 2. The results derived from fluorescence or spectrophotometric titrations agree, within the limits of experimental errors, with the data obtained by calorimetric measurements.

4. Discussion

Our results demonstrate that the binding of EH^+ both to CB8 and to EH^+–CB8 are enthalpically driven processes. Despite the 38-fold larger stability constant of the 1:1 complex, the inclusion of the first EH^+ is much less exothermic than the second binding step. Substantial entropy gain contributes to the driving force of 1:1 encapsulation, whereas 2:1 complexation is entropically highly unfavourable. The removal of high-energy water molecules from the apolar cavity of cucurbiturils was found to play a very important role in controlling the binding strength (33-36). The water network is moderately distorted in CB8 (34) and only a fraction of water is expelled by the inclusion of EH^+. Therefore, EH^+–CB8 formation is accompanied by a limited enthalpy diminution. The energy of the remnant water in EH^+–CB8 becomes higher because less optimized interactions among the encapsulated water molecules can be developed. Consequently, the release of water upon embedment of the second EH^+ results in more substantial enthalpy gain than 1:1 complexation. The transfer of water from the interior of CB8 and from the hydrate shell of EH^+ to the bulk leads to entropy enhancement. The entropy loss

due to the inclusion does not counterbalance this effect since the loose binding of EH^+ in the spacious CB8 causes relatively small entropy change. In contrast, EH^+ association with EH^+–CB8 results in tightly packed complex, in which the degrees of freedom of the constituents are highly restricted. Hence, $(EH^+)_2$–CB8 formation is accompanied by a significant entropy decrease. The considerably lower binding affinity of EH^+ to EH^+–CB8 compared with the encapsulation in CB8 originates from the very unfavourable entropy contribution to the driving force in the former process.

K_{11} for EH^+–CB8 formation is ca. 6-fold smaller than the corresponding quantity for the inclusion of berberine, an isoquinoline alkaloid, in CB8 (18). This difference arises from the slightly less negative ΔH_{11} and the smaller entropy gain for EH^+ complexation. About 50-fold lower K_{21} value is obtained for $(EH^+)_2$–CB8 (Table 1) compared to the analogous process of berberine.(18) Both ΔH_{21} and ΔS_{21} are significantly less negative in the case of EH^+, and the enthalpy term dominates to a lesser extent when this alkaloid produces 2:1 complex. The binding affinity of EH^+–CB8 to CB8 is low because of the electrostatic repulsion between the high electron density of oxygens at the portals of the two hosts. Much smaller driving force for 1:2 complexation compared with 1:1 association was also found when sanguinarine, a natural benzo[c]phenanthridine alkaloid, interacted with cucurbit[7]uril (17).

The results of the present study are in contrast to the conclusions of a former report on EH^+ confinement in CB8, which suggested only 1:1 complex formation (30). We found about 7.6-fold larger equilibrium constant for the 1:1 EH^+–CB8 inclusion complex formation than the 2.1×10^5 M^{-1} value published by Gavvala and coworkers (30). This discrepancy probably arises from the fact that the dimerization of EH^+ (32) and the encapsulation of two EH^+ in the cavity of

CB8 were not previously taken into account. The substantial variation of the fluorescence decay parameters is due to the change of the binding stoichiometry with host and guest concentrations.

Supplementary Information

Supplemental data for this article can be accessed http://

Acknowledgement

The authors very much appreciate the support of this work by the Hungarian Scientific Research Fund (OTKA, Grant K104201) and MedInProt Protein Science Research Synergy Program. Z. M. thanks the support of the János Bolyai Research Scholarship of the Hungarian Academy of Sciences.

References

(1) Walker, S.; Oun, R.; McInnes, F. J.; Wheate, N. J. *Isr. J. Chem.* **2011,** *51***,** 616-624.

(2) Ghosh, I.; Nau, W. M. *Adv. Drug Deliv. Rev.* **2012,** *64***,** 764-783.

(3) Shchepotina, E. G.; Pashkina, E. A.; Yakushenko, E. V.; Kozlov, V. A. *Nanotechnologies in Russia* **2011,** *6***,** 773-779.

(4) Macartney, D. H. *Isr. J. Chem.* **2011,** *51***,** 600-615.

(5) Ghale, G.; Ramalingam, V.; Urbach, A. R.; Nau, W. M. *J. Am. Chem. Soc.* **2011,** *133***,** 7528-7535.

(6) Bailey, D. M.; Hennig, A.; Uzunova, V. D.; Nau, W. M. *Chem. Eur. J.* **2008,** *14***,** 6069-6077.

(7) Megyesi, M.; Biczók, L.; Jablonkai, I. *J. Phys. Chem. C* **2008,** *112***,** 3410-3416.

(8) Ghale, G.; Nau, W. M. *Acc. Chem. Res.* **2014,** *47***,** 2150-2159.

(9) Uzunova, V. D.; Cullinane, C.; Brix, K.; Nau, W. M.; Day, A. I. *Org. Biomol. Chem.* **2010,** *8*, 2037-2042.

(10) Montes-Navajas, P.; Gonzalez-Bejar, M.; Scaiano, J. C.; Garcia, H. *Photochem. Photobiol. Sci.* **2009,** *8*, 1743-1747.

(11) Hettiarachchi, G.; Nguyen, D.; Wu, J.; Lucas, D.; Ma, D.; Isaacs, L.; Briken, V. *Plos One* **2010,** *5*, e10514.

(12) Zhao, Y. J.; Pourgholami, M. H.; Morris, D. L.; Collins, J. G.; Day, A. I. *Org. Biomol. Chem.* **2010,** *8*, 3328-3337.

(13) Zhao, Y. J.; Buck, D. P.; Morris, D. L.; Pourgholami, M. H.; Day, A. I.; Collins, J. G. *Org. Biomol. Chem.* **2008,** *6*, 4509-4515.

(14) Wang, R. B.; Macartney, D. H. *Org. Biomol. Chem.* **2008,** *6*, 1955-1960.

(15) Saleh, N.; Koner, A. L.; Nau, W. M. *Angew. Chem. Int. Ed.* **2008,** *47*, 5398-5401.

(16) Appel, E. A.; Rowland, M. J.; Loh, X. J.; Heywood, R. M.; Watts, C.; Scherman, O. A. *Chem. Commun.* **2012,** *48*, 9843-9845.

(17) Miskolczy, Z.; Megyesi, M.; Tárkányi, G.; Mizsei, R.; Biczók, L. *Org. Biomol. Chem.* **2011,** *9*, 1061–1070.

(18) Miskolczy, Z.; Biczók, L. *Phys. Chem. Chem. Phys.* **2014,** *16*, 20147-20156.

(19) Miskolczy, Z.; Biczók, L. *J. Phys. Chem. B* **2014,** *118*, 2499-2505.

(20) Pandrangi, S.; Chikati, R.; Chauhan, P.; Kumar, C.; Banarji, A.; Saxena, S. *Tumor Biol.* **2014,** *35*, 723-737.

(21) Pohlit, A. M.; Rocha e Silva, L. F.; Henrique, M. C.; Montoia, A.; Amorim, R. C. N.; Nunomura, S. M.; Andrade-Neto, V. F. *Phytomedicine* **2012,** *19*, 1049.

(22) Stiborová, M.; Frei, E. *Curr. Med. Chem.* **2014,** *21*, 575-591.

(23) Liu, J.; Xiao, Y.; Allen, C. *J. Pharm. Sci.* **2004,** *93*, 132-143.

(24) Fung, S. Y.; Yang, H.; Bhola, P. T.; Sadatmousavi, P.; Muzar, E.; Liu, M.; Chen, P. *Adv. Funct. Mater.* **2009,** *19***,** 74-83.

(25) Dodin, G.; Schwaller, M.-A.; Aubard, J.; Paoletti, C. *Eur. J. Biochem.* **1988,** *176***,** 371-376.

(26) Fung, S. Y.; Duhamel, J.; Chen, P. *J. Phys. Chem. A* **2006,** *110***,** 11446-11454.

(27) Miskolczy, Z.; Biczók, L. *J. Photochem. Photobiol. A: Chem.* **2006,** *182***,** 82-87.

(28) Miskolczy, Z.; Biczók, L.; Jablonkai, I. *Chem. Phys. Lett.* **2006,** *427***,** 76-81.

(29) Miskolczy, Z.; Biczók, L.; Jablonkai, I. *J. Phys. Chem. A* **2012,** *116***,** 899-900.

(30) Gavvala, K.; Sengupta, A.; Koninti, R. K.; Hazra, P. *J. Phys. Chem. B* **2013,** *117***,** 14099-14107.

(31) Megyesi, M.; Biczók, L. *J. Phys. Chem. B* **2010,** *114***,** 2814-2819.

(32) Miskolczy, Z.; Biczók, L. *Chem. Phys. Lett.* **2016,** *644*, 292-295.

(33) Nau, W. M.; Florea, M.; Assaf, K. I. *Isr. J. Chem.* **2011,** *51***,** 559-577.

(34) Biedermann, F.; Uzunova, V. D.; Scherman, O. A.; Nau, W. M.; De Simone, A. *J. Am. Chem. Soc.* **2012,** *134***,** 15318-15323.

(35) Biedermann, F.; Vendruscolo, M.; Scherman, O. A.; De Simone, A.; Nau, W. M. *J. Am. Chem. Soc.* **2013,** *135***,** 14879-14888.

(36) Biedermann, F.; Nau, W. M.; Schneider, H.-J. *Angew. Chem. Int. Ed.* **2014,** *53***,** 11158-11171.

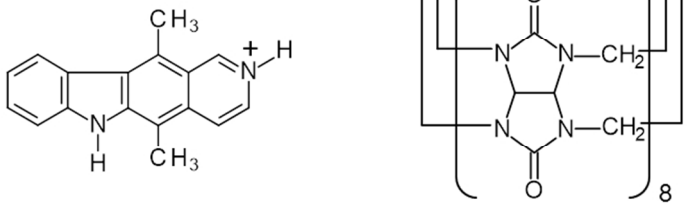

Protonated ellipticine (EH^+) Cucurbit[8]uril (CB8)

Figure 1. Chemical structure of the studied compounds
254x190mm (96 x 96 DPI)

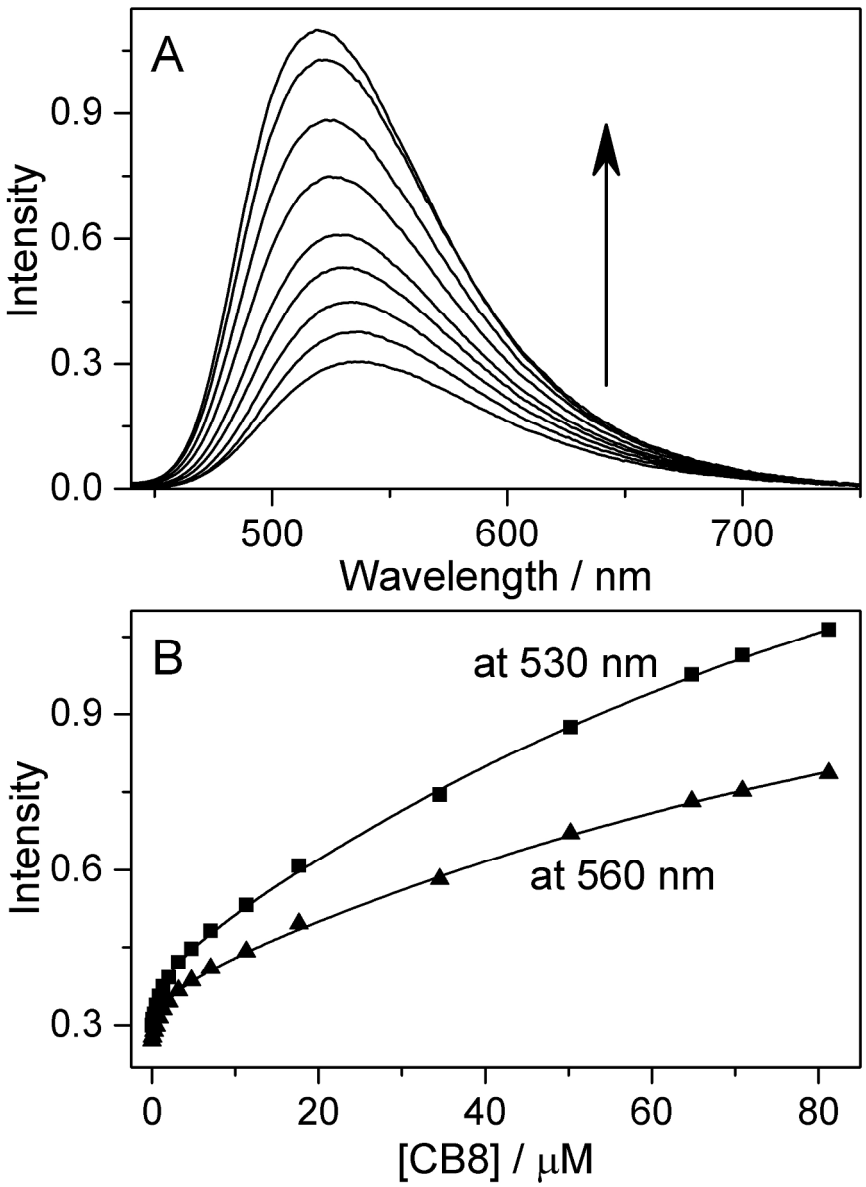

Figure 2. (A) Fluorescence spectra of 0.49 μM EH^+ in the presence of 0, 1.4, 4.7, 11, 18, 35, 50, 71 and 103 μM CB8 at pH 4. (Excitation at 422 nm) (B) Fluorescence intensity at 530 and 560 nm as a function of CB8 concentration. The lines represent the result of nonlinear least-squares fit.
201x264mm (300 x 300 DPI)

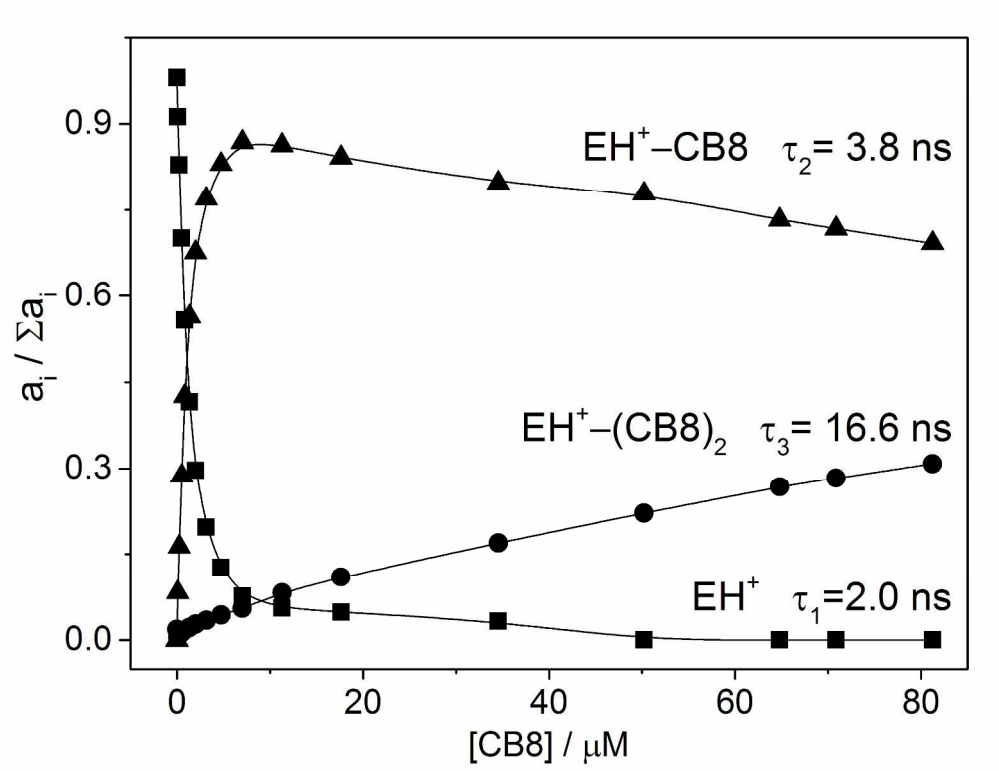

Figure 3. Effect of CB8 concentration on the amplitude fractions of the fluorescence decay components monitored at 590 nm in 0.49 μM EH^+ solution at pH 4.
269x207mm (300 x 300 DPI)

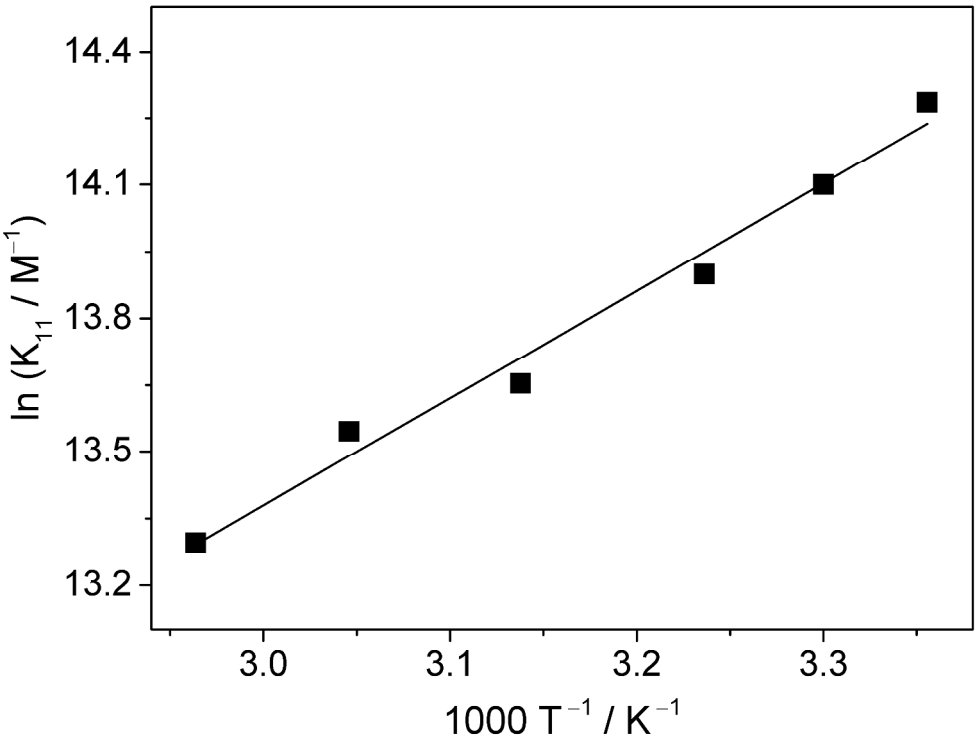

Figure 4. Logarithm of the binding constant of EH^+–CB8 complex formation as a function of the reciprocal temperature derived from fluorescence titration of 0.49 μM EH^+ solution with CB8 at pH 4.
258x201mm (300 x 300 DPI)

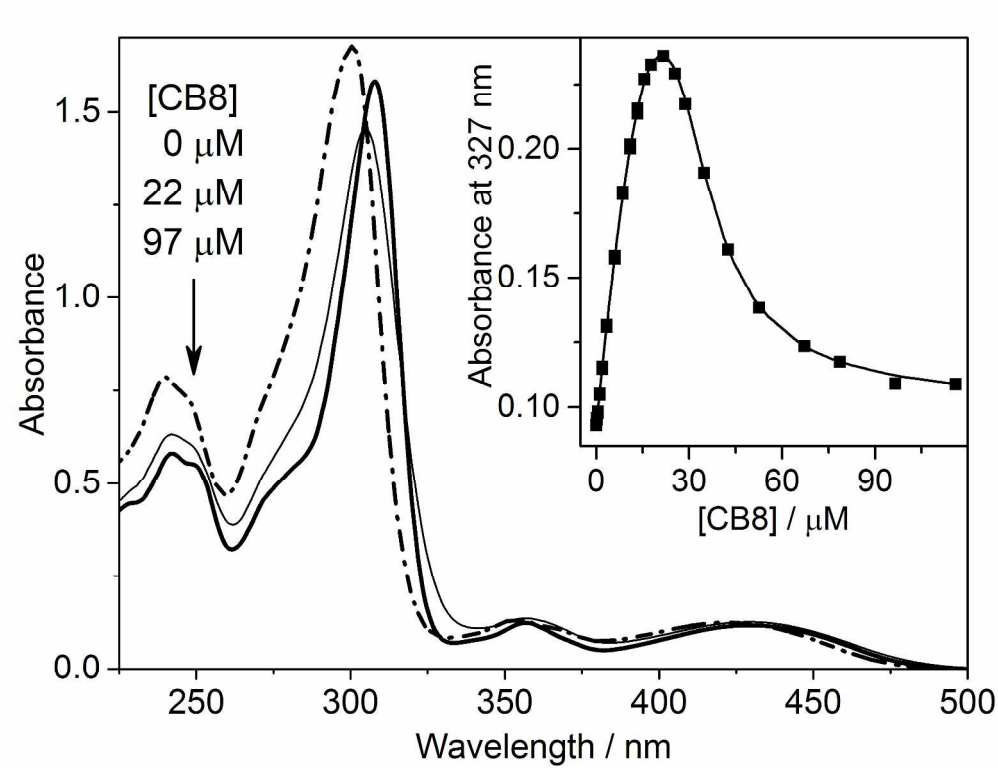

Figure 5. Absorption spectra of 37 μM EH^+ in the presence of 0, 22, and 97 μM CB8 at pH 4 (optical path 1 cm). Inset: absorbance change at 327 nm with CB8 concentration.
269x207mm (300 x 300 DPI)

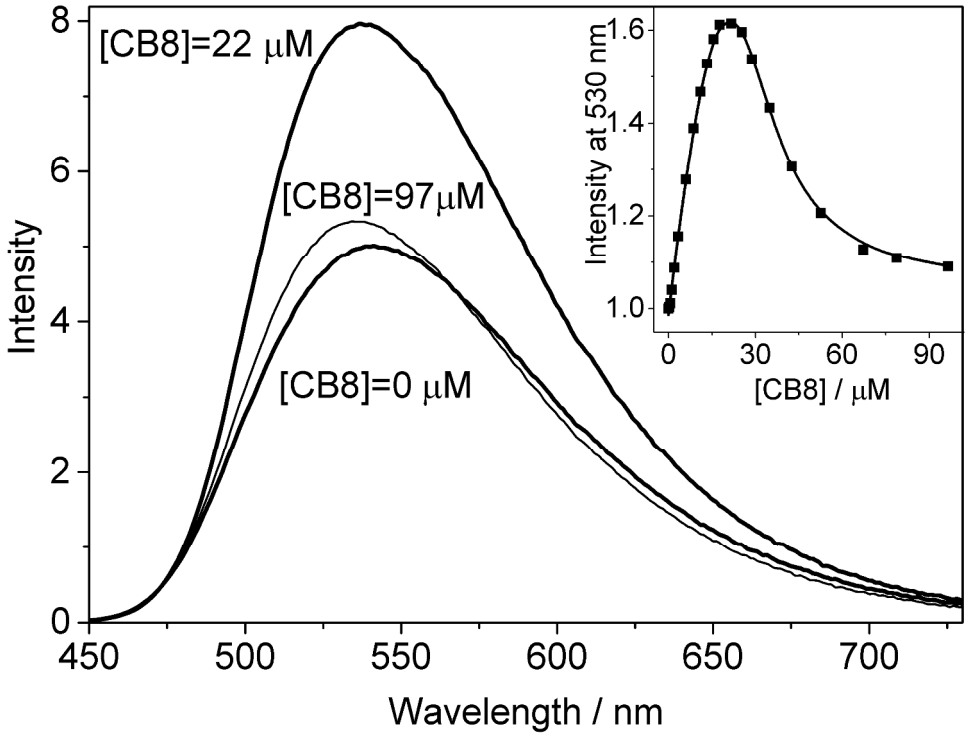

Figure 6. Fluorescence spectra of 37 μM EH^+ in the presence of 0, 22, and 97 μM CB8 at pH 4. (excitation at 372 nm) Inset: Fluorescence intensity at 530 nm versus CB8 concentration.
269x207mm (300 x 300 DPI)

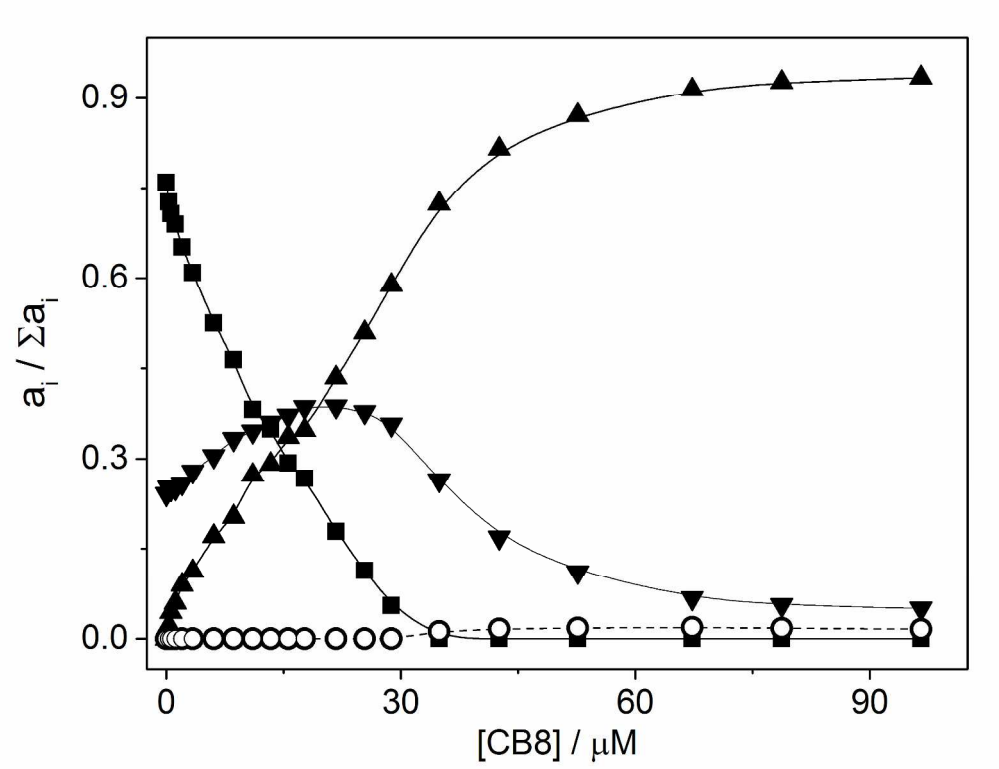

Figure 7. The amplitude fractions for the fluorescence decay components of 2.0 (■), 3.8 (▲), 7.5 (▼), and 16.6 ns (○) lifetimes as a function of CB8 concentration measured in 37 μM EH^+ solution at 530 nm.
269x207mm (300 x 300 DPI)

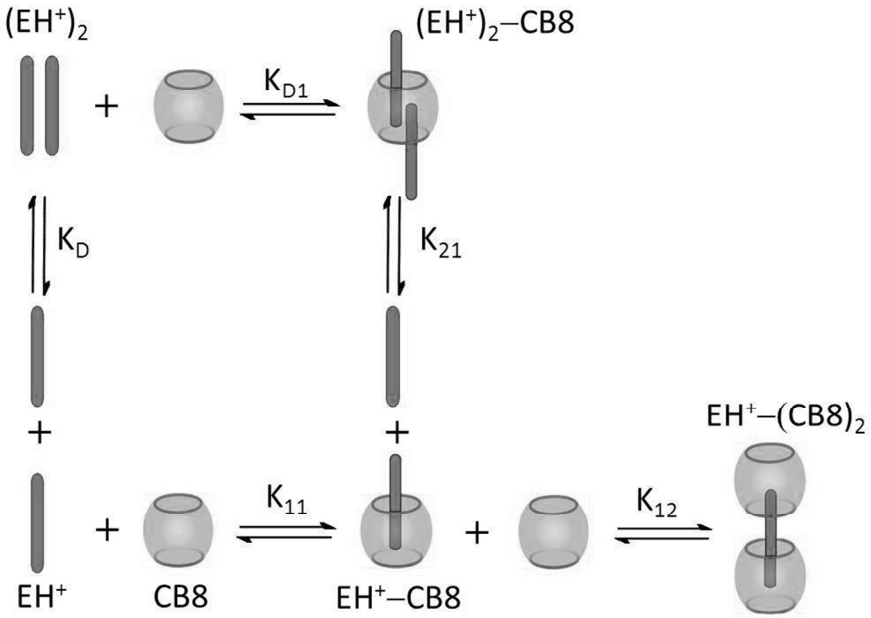

Figure 8. Association equilibriums
300x190mm (96 x 96 DPI)

Table 1. Association constants at pH 4 in water

K_{11} / 10^4 M^{-1}	K_{21} / 10^4 M^{-1}	K_D / 10^4 M^{-1}	K_{D1} / 10^4 M^{-1}	K_{12} / 10^4 M^{-1}
160 ± 20	4.2 ± 0.8	1.4 ± 0.3	520 ± 95	0.5 ± 0.4

Table 2. Thermodynamic parameters for EH^+–CB8 and $(EH^+)_2$–CB8 formation at 298 K

	From calorimetric measurements	From fluorescence or spectrophotometric titrations
ΔH_{11} / kJ mol^{-1}	–23 ± 3	–20 ± 3[a]
$T\Delta S_{11}$ / kJ mol^{-1}	12 ± 2	15 ± 2[a]
ΔS_{11} / J mol^{-1} K^{-1}	40 ± 7	51 ± 7[a]
ΔH_{21} / kJ mol^{-1}	–46 ± 6	–51 ± 5[b]
$T\Delta S_{21}$ / kJ mol^{-1}	–19 ± 5	–24 ± 4[b]
ΔS_{21} / J mol^{-1} K^{-1}	– 65 ± 17	–80 ± 14[b]

[a] From fluorescence titrations in 0.49 μM EH^+ solution. [b] From spectrophotometric titrations in 37 μM EH^+ solution.

Electronic Supplementary Information

Multiple inclusion complex formation of protonated ellipticine with cucurbit[8]uril: Thermodynamics and fluorescence properties

Zsombor Miskolczy,[a] László Biczók[a*], István Jablonkai[b]

[a]*Institute of Materials and Environmental Chemistry, Research Centre for Natural Sciences, Hungarian Academy of Sciences, P.O. Box 286, 1519 Budapest, Hungary*

[b]*Institute of Organic Chemistry, Research Centre for Natural Sciences, Hungarian Academy of Sciences, P.O. Box 286, 1519 Budapest, Hungary*

* Corresponding author. E-mail: biczok.laszlo@ttk.mta.hu

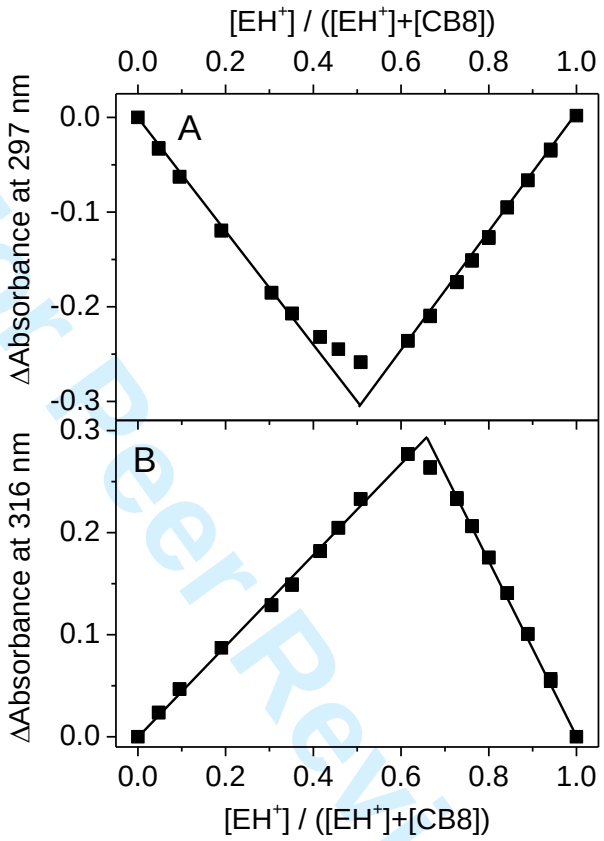

Figure S1 Job plot derived from spectrophotometric titration data at 297 (A) and 316 nm (B) keeping $[EH^+]+[CB8] = 76\ \mu M$ at pH 4 in water.

The absorbance change is due primarily to the contribution of the 1:1 and 2:1 guest:host complexes at 297 and 316 nm, respectively. Therefore, the Job plots presented at these wavelengths reflect the existence of two types of complexes. $EH^+–(CB8)_2$ has negligible contribution under the employed experimental condition.

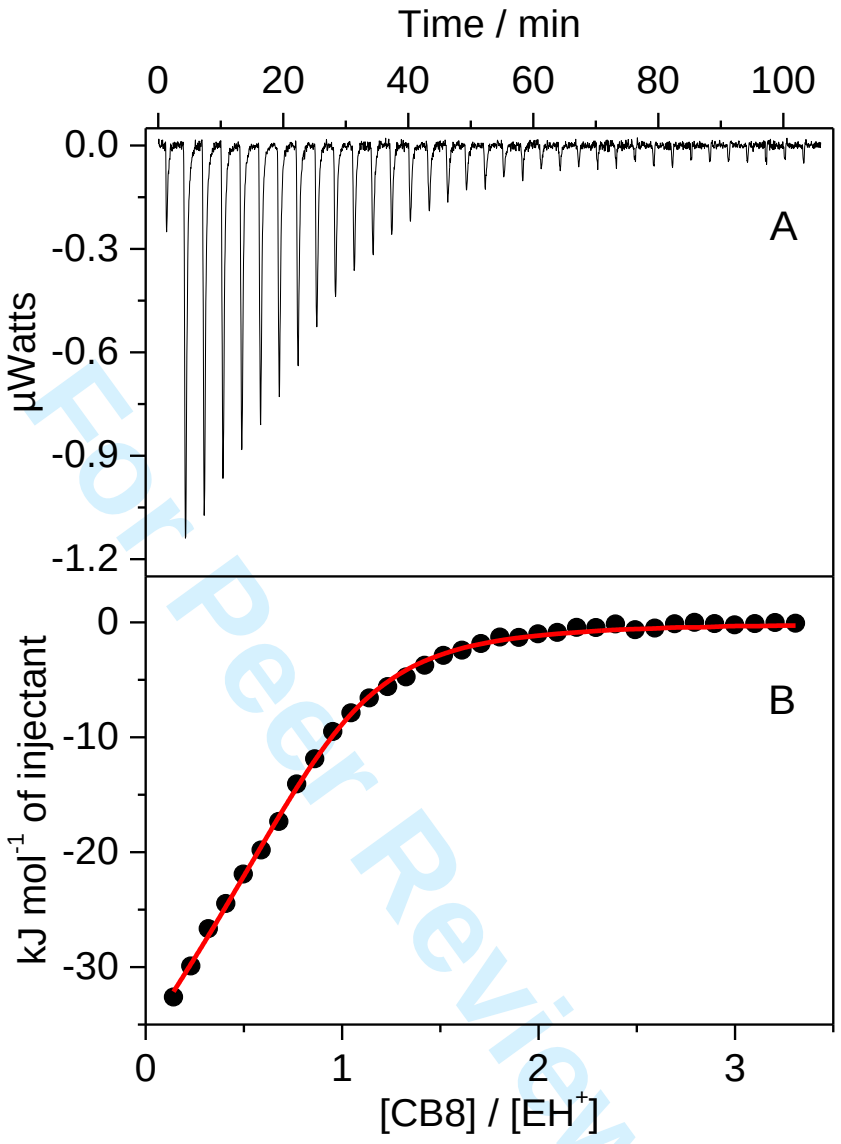

Figure S2 (A) Results of an isothermal calorimetric titration at pH 4 for the addition of 124 µM CB8 (8 µl per injection) to 8 µM EH^+ at 298 K. (B) The integrated heat evolved per injection after subtraction of the dilution heat of the ligand (●) as a function of [CB8]/[EH^+] molar ratio. The line represents the nonlinear least-squares fit with a stepwise binding to two sites model.

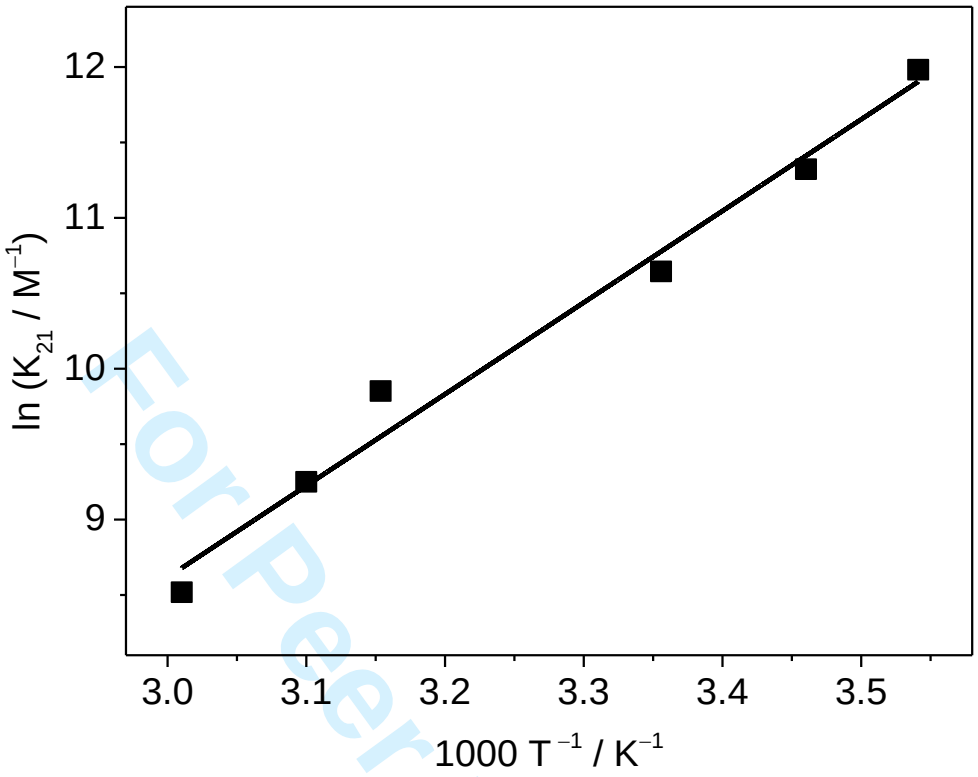

Fig. S3 Logarithm of the binding constant of $(EH^+)_2$–CB8 complex formation as a function of the reciprocal temperature derived from spectrophotometric titration of 37 μM EH^+ solution with CB8 at pH 4. The analysis of the experimental data with a relationship analogous to eq 8 provided $\Delta H_{21} = -51 \pm 5$ kJ mol^{-1} and $\Delta S_{21} = -80 \pm 14$ J mol^{-1} K^{-1}.

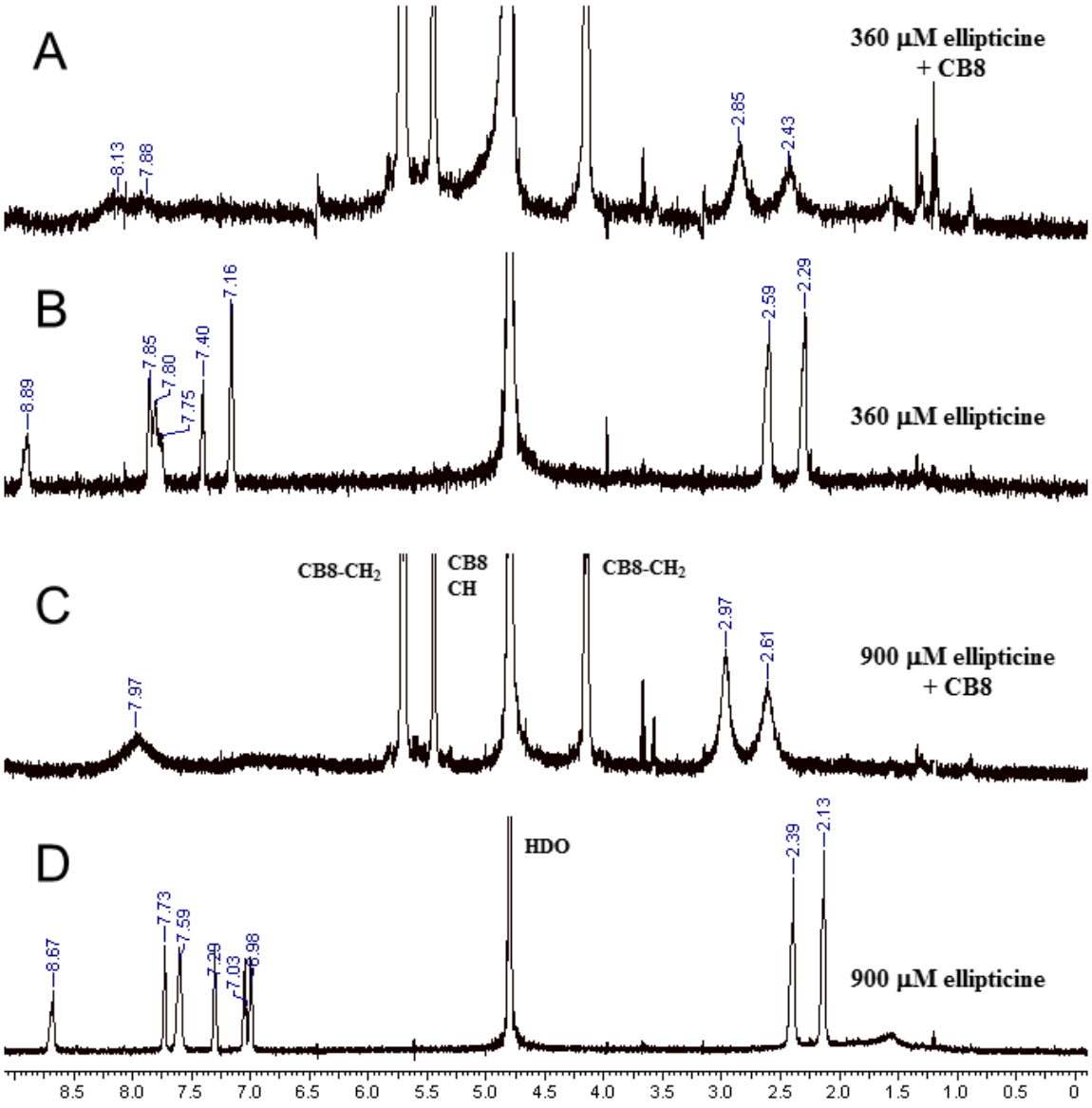

Figure S4 ^{1}H NMR spectra of (A) 360 μM EH^+ and 190 μM CB8 mixture, (B) 360 μM EH^+, (C) 900 μM EH^+ and 190 μM CB8 mixture, (D) 900 μM EH^+ in 100 μM DCl D_2O solutions at 296 K. NMR experiments were performed on a Varian NMR System (600 MHz for 1H) spectrometer.

Figure S4 (B) and (D) present the concentration dependence of 1H NMR spectra of EH^+. The increase of EH^+ concentration from 360 to 900 μM triggered upfield shifts of both methyl and

aromatic protons due to the increase of $(EH^+)_2$ dimer concentration [32]. Addition of 190 μM CB8 to EH^+ solution (Figure S4 A and C) brought about broadening and downfield shifts of the methyl proton signals. The resonances of the aromatic protons became even broader suggesting that the rate of exchange between bound and free EH^+ was probably comparable to the NMR timescale.

Derivation of equation 4

Equation 4 was obtained on the basis of the association equilibria presented in Scheme 2.

$$K_D = [(EH^+)_2]/([EH^+][EH^+]) \quad \text{(S1)}$$

$$[(EH^+)_2] = K_D[EH^+][EH^+] \quad \text{(S2)}$$

$$K_{21} = [(EH^+)_2 - CB8]/([EH^+ - CB8][EH^+]) \quad \text{(S3)}$$

$$[(EH^+)_2 - CB8] = K_{21}[EH^+ - CB8][EH^+] \quad \text{(S4)}$$

$$K_{D1} = [(EH^+)_2 - CB8]/([(EH^+)_2][CB8]) \quad \text{(S5)}$$

The substitution of eqs S2 and S4 into eq S5 yields

$$K_{D1} = K_{21}[EH^+ - CB8][EH^+]/(K_D[EH^+][EH^+][CB8]) \quad \text{(S6)}$$

$$K_{D1} = K_{21}[EH^+ - CB8]/(K_D[EH^+][CB8]) \quad \text{(S7)}$$

Using the definition of K_{11}:

$$[EH^+ - CB8]/([EH^+][CB8]) = K_{11} \quad \text{(S8)}$$

eq S7 leads to

$$K_{D1} = K_{21}K_{11}/K_D \quad \text{(S9)}$$